

High-Pressure Powder Diffraction on Synchrotron Sources

R. J. Nelmes and M. I. McMahon

Department of Physics and Astronomy, The University of Edinburgh, Mayfield Road, Edinburgh EH9 3JZ, UK

(Received 29 April 1994; accepted 10 June 1994)

The sample volume in diamond-anvil pressure cells suitable for X-ray powder diffraction studies is very small ($\leq 100\ \mu\text{m}$ across). The resulting low signal-to-noise ratio has made it very difficult to obtain useful results with monochromatic angle-dispersive techniques, and the alternative white-beam energy-dispersive techniques have limited resolution and generally give unreliable peak intensities. The situation has been transformed recently by the introduction of the image-plate two-dimensional detector, which allows angle-dispersive methods to be used with a greatly increased signal and improved powder averaging. A short review is given of this development, the experimental techniques, and the principal advantages, particularly as found in results obtained at SRS Daresbury over the past two or three years.

Keywords: high-pressure diffraction; powder diffraction; image-plate techniques.

Introduction

Experimentally accessible pressures have dramatic effects on physical properties, and bring about a rich variety of transitions and structures in all simple systems. This makes pressure a powerful probe of our understanding of condensed matter, and studies of high-pressure phenomena have stimulated an extensive literature of theoretical and computational work. The behaviour of matter under very high compression is also of central importance to the whole field of earth and planetary science – over 90% of the mass of our solar system is at pressures above (much of it greatly above) 10 GPa. And pressure has long played a major role in applications such as the synthesis of new hard materials. All of these activities require a foundation of accurate structural information, but this has always proved relatively difficult to obtain.

Now, some new developments in experimental techniques on synchrotron sources are allowing significant progress to be made in the quality of crystal structure information at high pressure. Though very exciting prospects are opening up for single-crystal work, the most fully developed advances so far have been made in powder diffraction. In any case, high-pressure diffraction studies often require powder techniques because single crystals fail to survive the large density changes that accompany many pressure-induced phase transitions. Some powder diffraction work is performed with so-called 'large-volume' devices. So far these have required very large (and massive) presses to take a sample volume of a few mm^3 to some 20 GPa (but see Besson, Hamel, Grima, Nelmes, Loveday, Hull & Häusermann, 1992), and their use has generally been restricted to specialist applications such as combined high-pressure and very high-temperature studies. By far the greatest amount of high-pressure structural research has been done with diamond-anvil pressure cells (DACs),

which are relatively easy to use and can reach pressures above 100 GPa.

In a DAC, the sample and a pressure-transmitting fluid are contained in a small hole ($\leq 200\ \mu\text{m}$ across) in a thin metal foil, or gasket, placed between the flat tips of two gem-quality diamonds. Pressure is applied by squeezing the diamonds together, usually using a piston–cylinder arrangement. The effective sample volume is very small – of the order of only $100\ \mu\text{m}$ in diameter and $50\ \mu\text{m}$ thick, or even somewhat less if the highest pressures are required. This results in the relatively weak signal that characterizes all high-pressure diffraction experiments, and accounts for the choice of energy-dispersive (ED) techniques for most of the work performed on synchrotron sources over the last decade or so. The full 'white' beam more than compensates for the limited sample volume and makes it possible to use much smaller samples and thus reach considerably higher pressures than in earlier laboratory-based work. However, ED techniques suffer from relatively poor resolution, unavoidable contaminant features such as sample-fluorescence lines, and poor powder averaging due to the high degree of collimation required between the sample and the detector. This has resulted in intensities that are generally unreliable, and has made it difficult to detect structural subtleties and to perform structure refinements.

This situation has been transformed recently by the introduction of the image-plate (IP) area detector, used with monochromatic synchrotron radiation for angle-dispersive (AD) studies. The characteristics of the IP overcome all the principal limitations of working with photographic film. The IP is highly sensitive to the short ($\leq 0.7\ \text{\AA}$) wavelengths needed to penetrate pressure cells, the dynamic range of $\sim 10^5$ is about three orders of magnitude better than film, and the very low intrinsic noise level of the

IP is some 300 times less than the intrinsic chemical fog level of film. The sensitivity, high dynamic range and low intrinsic noise level of the IP are almost ideally suited to the collection of AD powder diffraction data at high pressure, where the ultimate limits are set by both signal and signal-to-background. Most importantly, the fact that the IP is a two-dimensional detector means that a substantial portion of the Debye–Scherrer rings can be intercepted and collected; subsequent integration around the powder rings greatly increases the signal-to-noise ratio and also much improves the powder averaging. The resulting one-dimensional profile is then suitable for least-squares refinement of atomic coordinates, using standard Rietveld techniques (Rietveld, 1969). This short review focuses on the recent advances in AD powder diffraction with DACs and an image-plate detector. [The reader is referred to Häusermann (1992), and work cited therein, for information on some other recent developments in high-pressure powder diffraction on synchrotron sources.]

The use of image plates for high-pressure powder diffraction was pioneered at the Photon Factory in Japan (Shimomura, Takemura, Fujihisa, Fujii, Ohishi, Kikegawa, Amemiya & Matsushita, 1992), but the techniques have been significantly further developed during the last three years at SRS Daresbury (UK) (Nelmes, Hatton, McMahan, Piltz, Crain, Cernik & Bushnell-Wye, 1992; Nelmes, McMahan, Hatton, Piltz, Crain, Cernik & Bushnell-Wye, 1992). Substantial gains in data quality have been obtained (i) by the use of conical-aperture DACs (originally designed for single-crystal diffraction studies) to allow the full two-dimensional Debye–Scherrer pattern to be collected; (ii) by developing shielding, collimation and alignment techniques that remove all non-sample scattering and minimize the general background level; and (iii) by developing interactive software for integrating the full two-dimensional images.

Experimental techniques

The principal components of the current SRS beamline equipment are shown in Fig. 1. A double-bounce channel-

cut Si(111) monochromator ($\Delta\lambda/\lambda$ of $\sim 10^{-4}$), some 15 m from the 5 T superconducting wiggler magnet, is used to select the required wavelength, after which tungsten-carbide slits are used to reduce the monochromatic beam dimensions to $0.5 \times 0.5 \text{ mm}^2$. Lead shielding encloses the emerging beam until it is finally collimated to a circular beam 50–100 μm in diameter by a platinum pinhole. For wavelengths shorter than 0.4745 Å, the platinum *K* absorption edge at 0.1582 Å provides enhanced attenuation of the $\lambda/3$ harmonic in the incident beam, and this prevents contamination of the powder pattern by low-angle $\lambda/3$ lines from the pressure-cell gasket material. To align the sample accurately on the X-ray beam, an optical method is used – based on that employed at the Photon Factory (Shimomura, Takemura, Fujihisa, Fujii, Ohishi, Kikegawa, Amemiya & Matsushita, 1992). The telescope in Fig. 1 is for this purpose, and is removed during exposures. Experience at SRS has shown that, for reliable alignment, the optical axis of the telescope must be accurately parallel to the X-ray beam and perpendicular to the faces of the diamond anvils (through which the sample is viewed). The laser in Fig. 1 is used to ‘mark’ the X-ray beam, and align the components (to $<0.1^\circ$) by reflection from reference surfaces. This degree of optical alignment makes it possible to work reliably with a 75 μm diameter X-ray beam and samples in gasket holes as small as 100 μm across without any contaminant scattering from the gasket material.

Fig. 2 shows a typical two-dimensional image obtained with this equipment. The pattern is entirely free from contaminant lines and has a low uniform background. Pattern resolution is sometimes determined by the sample – broadening due to small particle size, strain or pressure gradients is quite common in high-pressure work. Otherwise the resolution is limited by the point-spread function (PSF) of the image-plate reader. At SRS, patterns are usually recorded on Kodak plates $20 \times 25 \text{ cm}^2$ in area (there is also an option of $35 \times 43 \text{ cm}^2$), and read on a Molecular Dynamics 400A PhosphorImager. This is an off-line system, which has distinct advantages of flexibility – for example, in making it possible to use different sample-to-plate distances and different plate sizes, and work with

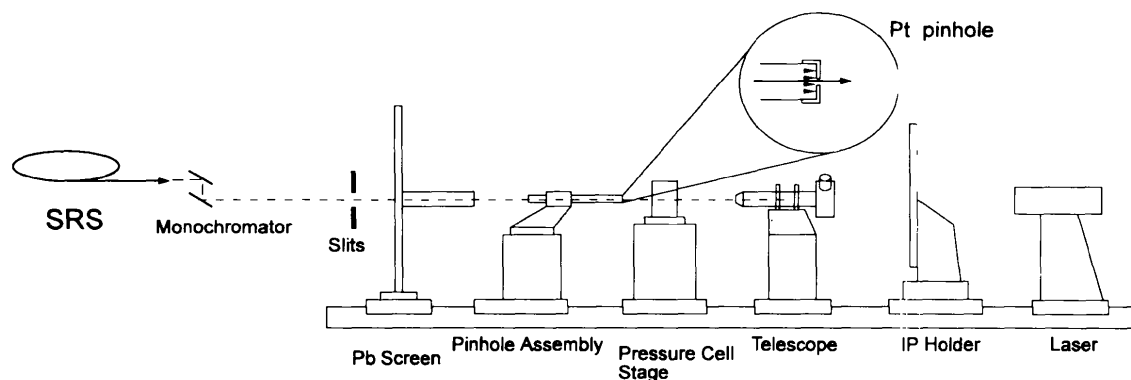


Figure 1

The beamline setup for high-pressure powder diffraction on station 9.1 at SRS Daresbury.

plates set off-centre or tilted. The standard pixel size is $88 \times 86 \mu\text{m}^2$, for which the reading time is ~ 10 min with the $20 \times 25 \text{ cm}^2$ plate. An option of $176 \times 176 \mu\text{m}^2$ pixels allows the same area to be scanned in only 2–3 min with a $\sim 40\%$ loss in signal. The PSF gives minimum peak widths (FWHM) of about five pixels (of the $88 \times 86 \mu\text{m}^2$ size), which corresponds to 0.08° in 2θ at a typical sample-to-plate distance of 350 mm. If this distance is doubled, a smaller part of the pattern can be recorded with a resolution of $\sim 0.05^\circ$ in 2θ , which approaches the performance of optimized high-resolution powder diffraction facilities (see, for example, Jephcoat, Finger & Cox, 1992). Fig. 3 is an integrated one-dimensional profile typical of the best resolution achieved in normal use of the equipment.

The *PLATYPUS* suite of programs, developed for integrating the two-dimensional images to one-dimensional profiles, has been described in detail previously (Piltz, McMahon, Crain, Hatton, Nelmes, Cernik & Bushnell-Wye, 1992). The principal steps are as follows. The centre of the diffraction pattern is located by fitting the image of the heavily attenuated direct beam, and the two-dimensional

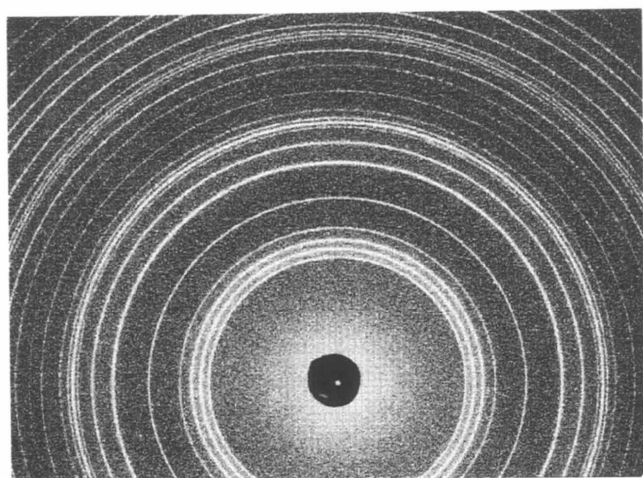


Figure 2
A two-dimensional image of CdS collected at 0.35 GPa. $\lambda = 0.4650 \text{ \AA}$. Exposure time = 21 min.

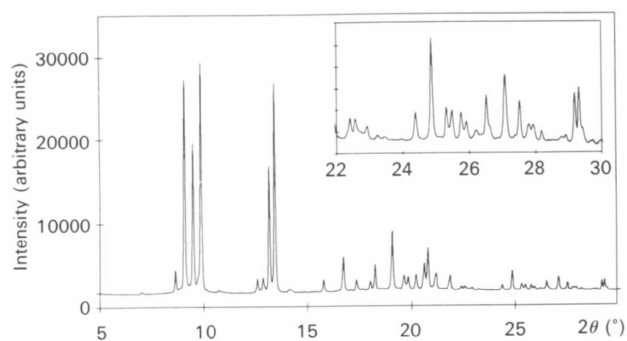


Figure 3
Integrated profile of InSb phase P4 at 3.5 GPa. $\lambda = 0.4446 \text{ \AA}$. Exposure time = 8.5 h. The inset shows an enlargement of the high-angle part of the pattern.

diffraction pattern is divided up into 30 sectors around this centre. Each sector is integrated along circular arcs to produce 30 one-dimensional profiles, and the tilts of the image plate away from being perpendicular to the primary beam are then refined such that these 30 individual powder profiles come into register, producing a summed profile that is maximally 'sharp'. The full two-dimensional image is then 'rebinned', taking account of the refined tilts, to give the final one-dimensional profile.

Discussion

It is clear that the quality of data obtainable with IP techniques is going to bring dramatic improvements to the level and quality of structural information on high-pressure phases – especially when coupled with the high brilliance of third-generation sources. For example, the Japanese group that pioneered the application of image plates to high-pressure powder diffraction is now attempting to determine electron-density changes as a function of pressure (Fujihisa, Fujii, Sakata, Takata, Kubota, Takemura & Shimomura, 1992). This would have been a completely impossible goal only a short time ago. The most important aspects of the new techniques appear to be the access to two-dimensional information, the high sensitivity to weak signals, and the reliable peak intensities resulting from the pattern integration, coupled with good resolution and speed of data collection. These principal features of image-plate data are now briefly discussed and illustrated.

The ability to record full Debye–Scherrer patterns, through the use of conical-aperture DACs, brings many advantages in addition to those arising from pattern integration. For example, it is possible to see and interpret crystallization effects such as those shown for InSb in Fig. 4, or to detect any intensity variations that occur around the rings as a result of preferred orientation or other sample inhomogeneities. Indeed, very recent work at SRS suggests that it is going to prove crucial to use two-dimensional

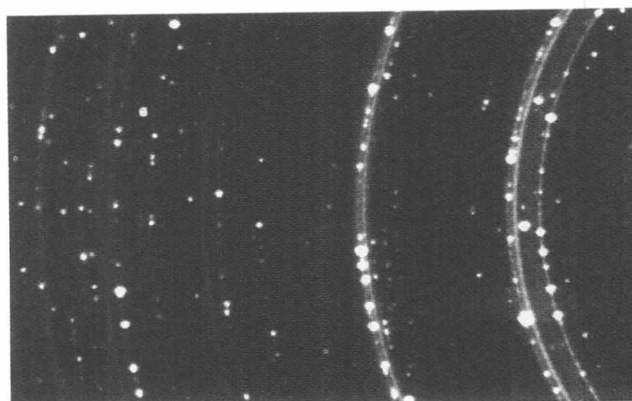


Figure 4
Part of a two-dimensional image of InSb phase P3 (smooth lines) recrystallizing to phase P4 (spotty lines) at 3.5 GPa. $\lambda = 0.4442 \text{ \AA}$. Exposure time = 24 min.

information routinely in order to determine preferred orientation distributions prior to structure solution and refinement. In addition, it is often possible to distinguish different phases by the appearance of their diffraction rings, which is proving valuable in analysing the mixed-phase patterns commonly encountered under pressure.

The high sensitivity of the image plates, combined with the substantial improvement in signal-to-noise ratio achieved by the integration process, allows all but the very weakest of diffraction features to be observed in the integrated profiles. This sensitivity has, for example, made it possible to observe the very weak, so-called ‘difference’ reflections in InSb – resulting from out-of-phase scattering of the In and Sb atoms – and exploit anomalous-dispersion effects to determine the atomic ordering, or lack of it, in the high-pressure phases (Nelmes, McMahon, Hatton, Crain & Piltz, 1993). Fig. 5 shows a similar, more recent, study

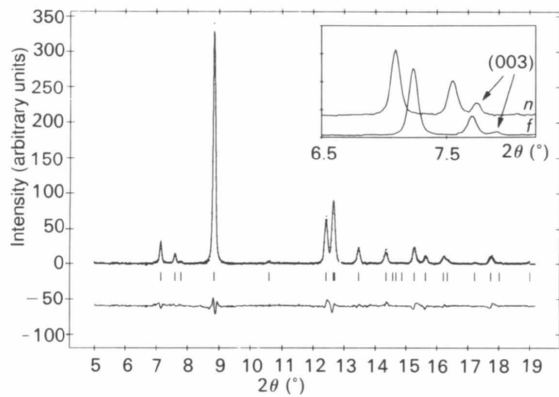


Figure 5

Rietveld refinement fit to a profile of CdTe cinnabar collected at 3.48 GPa. The tick marks show the positions of all reflections allowed by symmetry. The difference between observed and calculated profiles is displayed below the tick marks. The inset shows the weak (003) difference reflection recorded at 26.18 keV, far (*f*) from the Cd *K*-edge, and at 26.66 keV, near (*n*) to the Cd *K*-edge (at 26.72 keV).

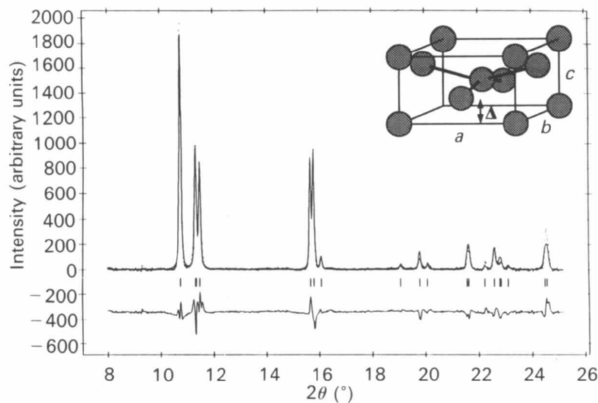


Figure 6

Rietveld refinement fit to a profile of silicon in the *Imma* phase at 14 GPa. The tick marks and difference profile are explained in the caption to Fig. 5. The inset shows the *Imma* crystal structure, which has one variable atomic coordinate, labelled Δ .

of the cinnabar phase of CdTe: the weak (003) difference reflection clearly increases in intensity as the Cd *K*-edge is approached – showing the structure to be site-ordered (Nelmes, McMahon, Wright & Allan, 1993; McMahon, Nelmes, Wright & Allan, 1993).

The improved resolution afforded by AD techniques was crucial to the unexpected discovery that silicon has an orthorhombic phase (space group *Imma*) between the well-known tetragonal β -tin Si-II and simple hexagonal Si-V phases (McMahon & Nelmes, 1993). The crystal structure of the *Imma* phase is shown as an inset in Fig. 6. Previous ED studies of silicon in this pressure region had missed the phase because the orthorhombic splittings – seen, for example, at $2\theta = 11.3$ and 15.7° in Fig. 6 – could not be resolved. Improved resolution also facilitates the interpretation of mixed-phase profiles, and increases the detectability of weak peaks.

The improvement to powder averaging brought about by integration leads to good reproducibility of peak intensities from exposure to exposure within the same sample, and generally between different samples of the same material. This accuracy in intensities, coupled with good pattern resolution, makes it possible to follow subtle structural changes with pressure, using full-profile (Rietveld) refinement methods, as shown in Fig. 7 for the atomic coordinate Δ of the *Imma* phase of silicon (McMahon, Nelmes, Wright & Allan, 1994).

Finally, amongst the characteristics discussed here, there is the speed with which the IP system is able to collect high-quality diffraction patterns. Although data-collection times are not as rapid as with ED techniques, in which the diffraction pattern from strongly scattering materials can be obtained in seconds, the IP system makes it possible to collect high-quality AD diffraction patterns in exposure times of 15–30 min for all but the most weakly scattering materials. This was indispensable in recent studies of the metastable BC8 phase of Ge, which is obtained by rapidly depressurizing Ge from ~ 14 GPa, but transforms quickly at atmospheric pressure to another, possibly hexagonal structure. Fig. 8 shows a clean, single-phase pattern of BC8-Ge obtained within 30 min of pressure release. This

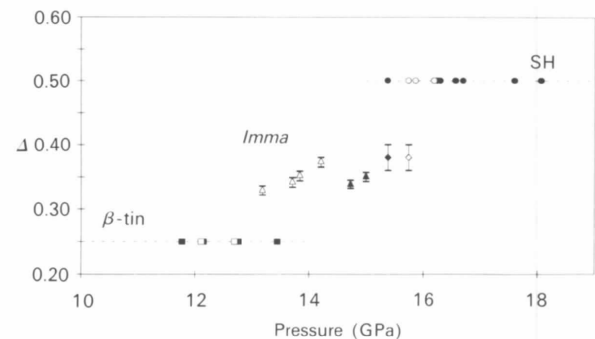


Figure 7

The pressure dependence of the atomic coordinate Δ in the β -tin, *Imma* and simple hexagonal (SH) phases of silicon. Δ is fixed by symmetry at 0.25 in the β -tin phase and 0.5 in the SH phase.

has allowed the first ever structure refinement of BC8-Ge to be carried out successfully (Nelmes, McMahon, Wright, Allan & Loveday, 1993).

Conclusions

The advantages of two-dimensional data collection in high-pressure powder diffraction are clear and exciting, and image-plate facilities are now being introduced for this purpose at other synchrotron sources such as CHESS, HasyLab and SSRL. [The large gains in effective signal and signal-to-background are also allowing some successful work to be performed on laboratory sources (Akahama, Kobayashi & Kawamura, 1993).] Further possibilities are in view with the development of different two-dimensional detectors offering real-time readout, and with the large gains in brilliance that will come from third-generation sources (Moy, 1993; Häusermann, 1993). Amongst other things, it should be possible to reach considerably higher pressures, study more weakly scattering materials, follow transition processes, and extend the techniques to liquid and amorphous samples. The future looks very bright for high-pressure structural studies on synchrotron sources.

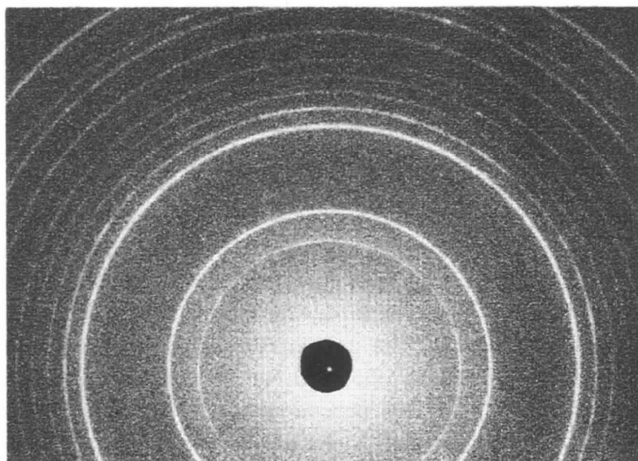


Figure 8

A two-dimensional image of the BC8 phase of germanium, collected within 30 min of forming the phase. $\lambda = 0.4654 \text{ \AA}$. Exposure time = 16 min.

We gratefully acknowledge the assistance of N. G. Wright, D. R. Allan, J. S. Loveday, A. A. Nield and G. Bushnell-Wye in various aspects of the experimental work, and the support of research grants from SERC and facilities made available by Daresbury Laboratory. Valued assistance with the maintenance and development of pressure cells has been given by D. M. Adams of Diacell Products.

References

- Akahama, Y., Kobayashi, M. & Kawamura, H. (1993). *Phys. Rev. B*, **48**, 6862–6864.
- Besson, J. M., Hamel, G., Grima, T., Nelmes, R. J., Loveday, J. S., Hull, S. & Häusermann, D. (1992). *High Press. Res.* **8**, 625–630.
- Fujihisa, H., Fujii, Y., Sakata, M., Takata, M., Kubota, Y., Takemura, K. & Shimomura, O. (1992). *Proceedings of AIRAPT XIII: Recent Trends in High-Pressure Research*, edited by A. K. Singh, pp. 145–147. Oxford: Oxford and IBH Publishing.
- Häusermann, D. (1992). *High Press. Res.* **8**, 723–737.
- Häusermann, D. (1993). *ESRF Newsl.* (18), 4–5.
- Jephcoat, A. P., Finger, L. W. & Cox, D. E. (1992). *High Press. Res.* **8**, 667–676.
- McMahon, M. I. & Nelmes, R. J. (1993). *Phys. Rev. B*, **47**, 8337–8340.
- McMahon, M. I., Nelmes, R. J., Wright, N. G. & Allan, D. R. (1993). *Phys. Rev. B*, **48**, 16246–16251.
- McMahon, M. I., Nelmes, R. J., Wright, N. G. & Allan, D. R. (1994). *Phys. Rev. B*, **50**, 739–743.
- Moy, J. P. (1993). *ESRF Newsl.* (18), 8–9.
- Nelmes, R. J., Hatton, P. D., McMahon, M. I., Piltz, R. O., Crain, J., Cernik, R. J. & Bushnell-Wye, G. (1992). *Rev. Sci. Instrum.* **63**, 1039–1042.
- Nelmes, R. J., McMahon, M. I., Hatton, P. D., Crain, J. & Piltz, R. O. (1993). *Phys. Rev. B*, **47**, 35–54; **48**, 9949–9952.
- Nelmes, R. J., McMahon, M. I., Hatton, P. D., Piltz, R. O., Crain, J., Cernik, R. J. & Bushnell-Wye, G. (1992). *High Press. Res.* **8**, 677–684.
- Nelmes, R. J., McMahon, M. I., Wright, N. G. & Allan, D. R. (1993). *Phys. Rev. B*, **48**, 1314–1317.
- Nelmes, R. J., McMahon, M. I., Wright, N. G., Allan, D. R. & Loveday, J. S. (1993). *Phys. Rev. B*, **48**, 9883–9886.
- Piltz, R. O., McMahon, M. I., Crain, J., Hatton, P. D., Nelmes, R. J., Cernik, R. J. & Bushnell-Wye, G. (1992). *Rev. Sci. Instrum.* **63**, 700–703.
- Rietveld, H. M. (1969). *J. Appl. Cryst.* **2**, 65–71.
- Shimomura, O., Takemura, K., Fujihisa, H., Fujii, Y., Ohishi, Y., Kikegawa, T., Amemiya, Y. & Matsushita, T. (1992). *Rev. Sci. Instrum.* **63**, 967–973.